



Photo-Induced Shrinking of Aqueous Glycine Aerosol Droplets

Shinnosuke Ishizuka,^{a,b,c,†,*} Oliver Reich,^{a,‡} Grégory David,^a and Ruth Signorell^{a*}

^a Laboratory of Physical Chemistry, ETH Zurich, Vladimir-Prelog-Weg 2, CH-8093, Zurich, Switzerland

^b Institute of Advanced Research, Nagoya University, Nagoya 046-8601, Japan

^c Institute of Space-Earth Environmental Research, Nagoya University, Nagoya 046-8601, Japan

ABSTRACT: Due to their small size, micrometer and submicron sized solution droplets can respond differently to physical and chemical processes compared with extended bulk material. Using optically trapped micrometer sized aqueous glycine droplets, we demonstrate photo-induced degradation of glycine upon irradiation with visible light, even though molecular glycine does not absorb light in the near UV/vis range to any significant extent. This reaction is observed as photo-induced shrinking of the droplet, which we characterize by analyzing the elastic light scattering and the Raman spectrum of the droplet over the course of the reaction. We find the volume to shrink with a constant rate over the major part of the shrinking process. This indicates the presence of a rate limiting photo-catalyst, which we attribute to mesoscopic glycine clusters in the droplet solution. Our findings relate to previous reports of visible light absorption by photosensitizers. However, to the best of our knowledge, this is the first experimental evidence of a photochemical pathway facilitated by mesoscopic clusters. Light interaction with such mesoscopic photoactive molecular aggregates might be more important for aerosol photochemistry than previously anticipated.

* rsignorell@ethz.ch, ishizuka.shinnosuke@i.mbox.nagoya-u.ac.jp

‡ S.I. and O.R. contributed equally to this work.



1 1. INTRODUCTION

2 Aerosols, dispersions of solid and liquid particles in a gas, are ubiquitous in Earth's atmosphere and as such play
3 an important role for many atmospheric processes (Boucher et al., 2013; Pöschl and Shiraiwa, 2015). Size, chem-
4 ical composition, viscosity and thermodynamic phase of aerosol particles respond to their environment including
5 the surrounding gas species, temperature, humidity (Bones et al., 2012; Zieger et al., 2017; Tang et al., 1997;
6 Swietlicki et al., 2008) and light irradiation (Pöschl and Shiraiwa, 2015; Cremer et al., 2016; Walser et al., 2007;
7 Corral Arroyo et al., 2022). Particular attention has been paid to their chemistry distinct from that in the bulk, a
8 phenomenon possibly arising from high surface to volume ratio of aerosol particles and the accessibility to highly
9 supersaturated states (Altaf et al., 2016; Kucinski et al., 2019; Bzdek and Reid, 2017). Various chemical reactions
10 have been shown to be accelerated in microdroplets (Cremer et al., 2016; Lee et al., 2015; Girod et al., 2011),
11 with some reactions being exclusive to the droplet phase (Lee et al., 2019). These unique reactors can act as
12 medium for the birth, growth and degradation of atmospherically relevant particles (Ruiz-Lopez et al., 2020), and
13 be utilized for organic synthesis (Bain et al., 2017). Chemical processes in prebiotic aerosols have also been
14 proposed as potential mechanisms for the origin of life (Tervahattu et al., 2004). However, molecular processes
15 leading to the anomalous chemistry in micrometer and submicron aerosol particles are still largely unknown.
16 Although some processes may be ascribed to the discontinuous and asymmetric intermolecular interactions at the
17 particle surface (Ruiz-Lopez et al., 2020), the microphysical origins behind many of the aforementioned particle
18 specific phenomena are still not adequately explored.

19

20 Glycine is an amino acid that acts as precursor to proteins and fulfills a number of other biological functions
21 (Arnstein, 1954; Hall, 1998; Jackson, 1991). With its small size and simple structure, glycine often serves as a
22 proxy for other amino acids and physiologically relevant molecules, and as such has been studied extensively in
23 the past. It is generally accepted that molecular glycine does not absorb light in the near UV/vis range, similar to
24 other amino acids (Bhat and Dharmaprakash, 2002). However, it has been shown that their optical properties
25 change when glycine molecules arrange themselves into mesoscopic clusters (Terpugov et al., 2021). Further-
26 more, these formations respond to light irradiation in non-trivial ways which can be exploited to induce long range
27 order inside the glycine solution (Alexander and Camp, 2019; Sugiyama et al., 2012; Zaccaro et al., 2001; Garetz
28 et al., 2002) on a scale of up to millimeters (Yuyama et al., 2010). While these interactions have the potential to
29 change the optical properties of glycine ensembles significantly and to enable new photochemical reaction path-
30 ways, there has been little experimental evidence for such reactions so far.

31

32 In this work, we study the response of aqueous glycine droplets to irradiation by visible light. We observe the
33 shrinking of optically trapped micrometer sized glycine droplets, which can be unambiguously attributed to the
34 exposure to the trapping laser with wavelength 532 nm. To the best of our knowledge, this interaction has not
35 been reported before. We characterize it here with particular focus on the shrinking rate and its dependence on the
36 light intensity. To explain our results, we discuss possible reaction schemes based on the available experimental



37 data. Although further data is needed to elucidate the exact photochemical pathways of the observed reaction,
38 these findings demonstrate the existence of a photochemical reaction for molecules which previously have been
39 considered photochemically inert at visible wavelengths.

40

41



42 2. METHODS

43 Dual beam optical traps are widely used to confine and isolate single particles (Ashkin, 1997; Gong et al., 2018;
44 Čížmár et al., 2005; Esat et al., 2018; Reich et al., 2020). The counter-propagating tweezers (CPT) setup for
45 trapping aqueous glycine droplets is shown in Fig. 1 and consists of a continuous green laser beam (Novanta
46 Photonics Opus 532 6W), which is expanded and then split into two beams of equal power. These two beams are
47 aligned counter-propagating on a single axis and focused into the trapping cell, where a single droplet is trapped
48 between the two focii.

49

50 The droplets are generated from 1.0 M or 2.0 M aqueous solutions of glycine (purity $\geq 99\%$, Sigma-Aldrich
51 G7126) using a commercial atomizer (TSI 3076) with pressurized, humidified nitrogen gas (purity 5.0). A system
52 of copper tubings directs the spray of particles into the trapping cell, where the droplets agglomerate at the desig-
53 nated trapping position. The humidification of the nitrogen flow is necessary to ensure that the droplets reach the
54 trapping position in the liquid state. The trapping cell is filled with nitrogen gas (purity 5.0) and a steady nitrogen
55 flow formed by combining wet and dry nitrogen with adjustable flow ratios is used to control the relative humidity
56 (RH) in the cell. For the experiments reported here, the RH is set at $77 \pm 3\%$ well above the efflorescence RH of
57 glycine at approximately 55 % (Chan et al., 2005). At this RH, the droplet solution is supersaturated with an
58 estimated glycine concentration of 60 % in mass (Chan et al., 2005), corresponding to approximately 5 M. Tem-
59 perature and RH inside the trapping cell are monitored by a sensor (Sensirion SHT35) placed a few millimeters
60 away from the trapping position. When the agglomerated particle reaches a size of approximately 2-3 μm in radius,
61 the remainder of the droplets in the cell are flushed out with nitrogen for 20-30 minutes to ensure that only the
62 trapped droplet remains in the cell. After flushing, the power of the trapping laser is kept constant until the end of
63 the measurement.

64

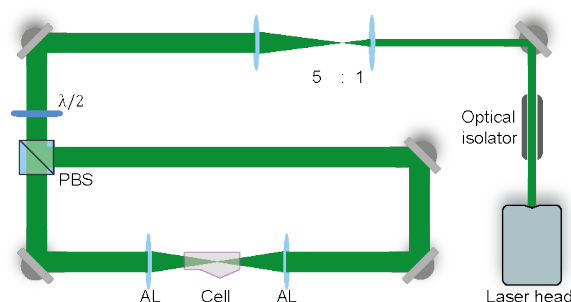
65 The particle shrinking is monitored by imaging the polarization resolved two-dimensional angular optical scatter-
66 ing (polarization resolved TAOS) of the particle (Parmentier et al., 2022), as shown in Fig. 2. The TAOS image
67 is obtained by collecting the elastically scattered light of the trapping beams under a scattering angle of $90 \pm 24^\circ$
68 with an objective (Mitutoyo 20x NA 0.42). The parallel and perpendicular polarization components with respect
69 to the scattering plane (TAOS PPol and TAOS SPol) are separated using a polarization beam splitter and recorded
70 with separate CMOS cameras (Thorlabs DCC1545M). The scattering intensity for each polarization is calculated
71 from the average of the respective TAOS image and recorded over time. At specific times, the shrinking spherical
72 particle reaches a size at which it is in resonance with the light of the trapping beams, which corresponds to a Mie
73 resonance (Bohren and Huffman, 2008). From the comparison of the recorded evolution of the polarization re-
74 solved scattering intensity to simulations using Mie theory, the size of the particle can be determined at the specific
75 times. Fig. 3 shows an example of such a TAOS analysis. The values of the size at the discrete points in time,
76 obtained from the times where the particles experience a Mie resonance, can then be interpolated with high accu-
77 racy to obtain the full size evolution of the particle over the course of the measurement.



78

79 The molecular composition of the particle is monitored by continuous recording of Raman spectra (David et al.,
80 2020) during the shrinking process. To this end, the light scattered by the particle is collected under a scattering
81 angle of $90 \pm 24^\circ$ by a second objective and fiber coupled into a low noise, high sensitivity spectrograph (Andor
82 KY-328i-A). The inelastically scattered light is analyzed in the range 540-680 nm which corresponds to Raman
83 shifts of 280-4100 cm^{-1} . This range contains in particular the O-H symmetric stretching mode of water ($\nu_2\text{-H}_2\text{O}$,
84 2700-3750 cm^{-1}) as well as several vibrational modes of glycine, which we exploit for the characterization of the
85 molecular composition (see later data for an example).

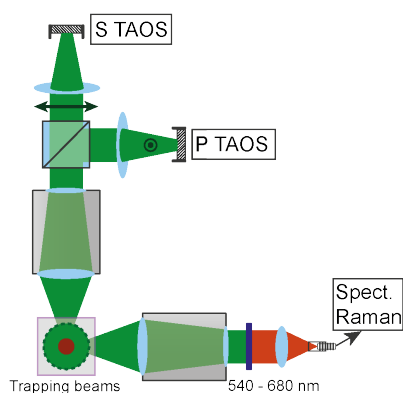
86



87

88 **Figure 1** Counter-propagating tweezers setup. The laser beam is first expanded by a factor of 5 and then split into
89 two beams by the polarizing beam splitter (PBS). The half-waveplate ($\lambda/2$) rotates the polarization to 45° with
90 respect to the axes of the PBS to ensure equal power splitting between the two beams. The beams are aligned on
91 a single axis and focused into the trapping cell using two aspherical lenses (AL). An optical isolator introduced
92 at the start of the beam path prevents unwanted optical feedback into the laser head.

93



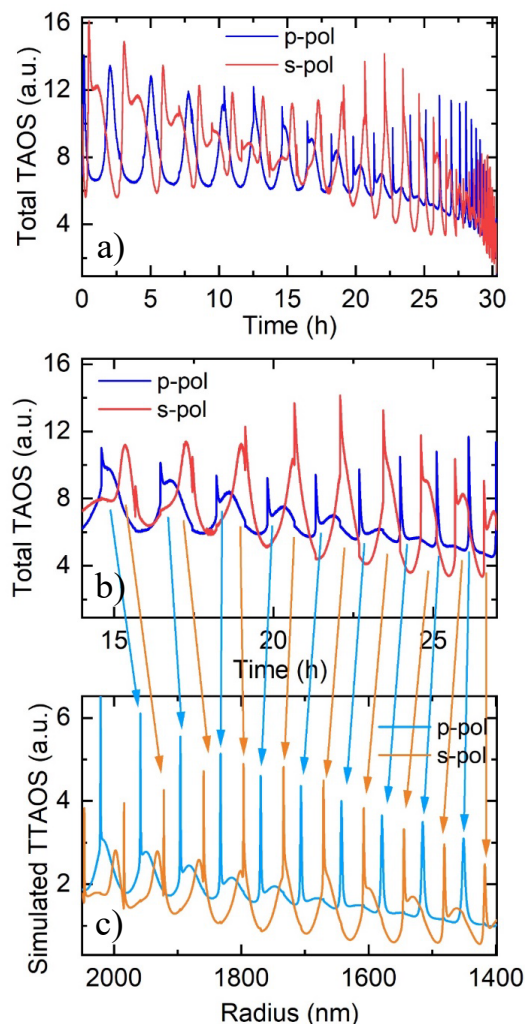
94

95 **Figure 2** Setup for TAOS imaging and Raman spectroscopy. The trapping beams run perpendicular to the figure
96 plane. The scattered light of the trapping beams is collected horizontally and vertically at a scattering angle of 90
97 $\pm 24^\circ$. The vertical beam is split into parallel and perpendicular polarized light with respect to the scattering plane



98 and the respective beam is loosely focused on a CMOS camera (P TAOS and S TAOS respectively). The hori-
99 zontal beam is filtered for the spectral range of 540 – 680 nm and fiber coupled into a low noise, high sensitivity
100 spectrometer (Spect. Raman) for measurement of the Raman spectrum.

101



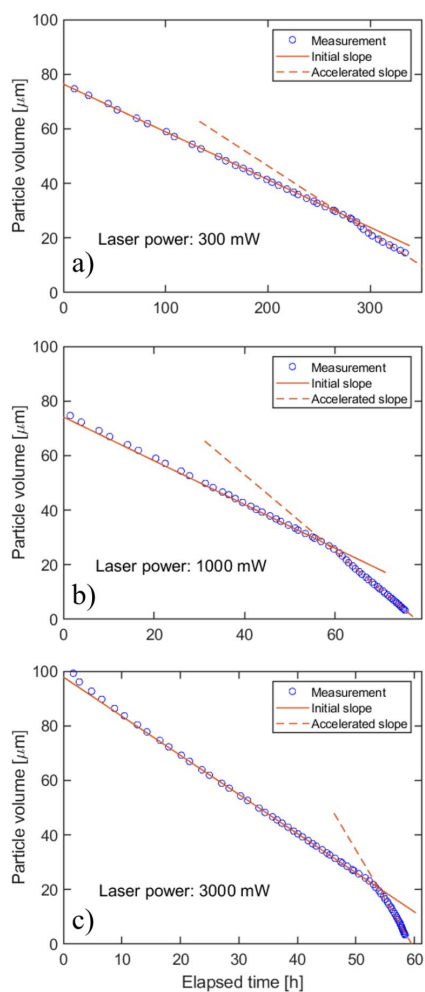
102

103 **Figure 3** Analysis of the two-dimensional angular optical scattering spectrum (TAOS). **a)** Experimental polariza-
104 tion resolved total TAOS signal over time. **b)** Zoom on a specific time interval for clarity **c)** Simulated polariza-
105 tion resolved total TAOS signal as function of particle radius in the specific time interval. Arrows indicate the
106 peak assignment based on the similarities between the peak shapes.

107

108 3. RESULTS AND DISCUSSION

109 The shrinking of the aqueous glycine droplets over time is shown in Fig. 4 for three representative examples. The
110 droplets are trapped using different laser powers, which affects the rate at which their volume is decreasing. For
111 all laser powers, the volume is observed to shrink linearly with time over a large portion of the shrinking process.
112 After a certain point ('point of acceleration'), when the droplet has lost 60 – 80 % of its volume, the shrinking
113 suddenly accelerates, only to continue again approximately linearly with time, albeit at a higher rate.

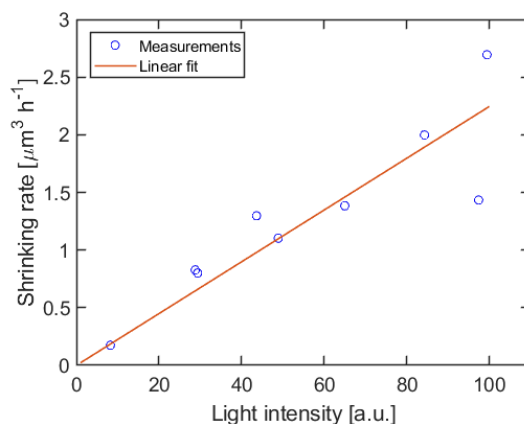


114

115 **Figure 4** Volume shrinking of glycine droplets as a function of time. **a)** Droplet trapped at 300 mW nominal laser
116 power **b)** droplet trapped at 1000 mW nominal laser power **c)** droplet trapped at 3000 mW nominal laser power.
117 At higher power, the shrinking proceeds faster (visible by the larger slopes). Solid and dashed lines indicate the
118 best linear fit before and after the acceleration of the shrinking observed at approximately **a)** 280 h, **b)** 59 h and
119 **c)** 53 h.



120 To quantify the dependence of the shrinking rate on the light intensity incident on the particle, a linear fit is
121 performed on the data before and after the point of acceleration. Since between different experiments, the align-
122 ment of the optical trap, and hence the focusing of the laser light on the particle, is subject to temporal mechanical
123 drifts, the nominal laser power used for trapping of the droplets is not an optimal indicator for the incident inten-
124 sity. Instead, we use the intensity of the scattered light as a measure that is proportional to the incident light
125 intensity. The intensity of the scattered light is obtained from the average signal of the TAOS PPol and SPol
126 images during the time of the droplet shrinking. To ensure consistency between the different experiments, the
127 average of the light intensity is taken over the same volume interval of $[65.4, 51.0] \mu\text{m}^3$ (radius $[2.5, 2.1] \mu\text{m}$) for
128 all droplets. This interval corresponds to the interval for which we obtained data for most droplets. Fig. 5 shows
129 the resulting initial shrinking rates as function of light intensity. The shrinking rate is observed to be proportional
130 to the light intensity, confirming that the shrinking is induced by the trapping laser at a wavelength of 532 nm.



131

132 **Figure 5** Fitted shrinking rate as function of light intensity. The solid line indicates the best linear fit through
133 the origin.

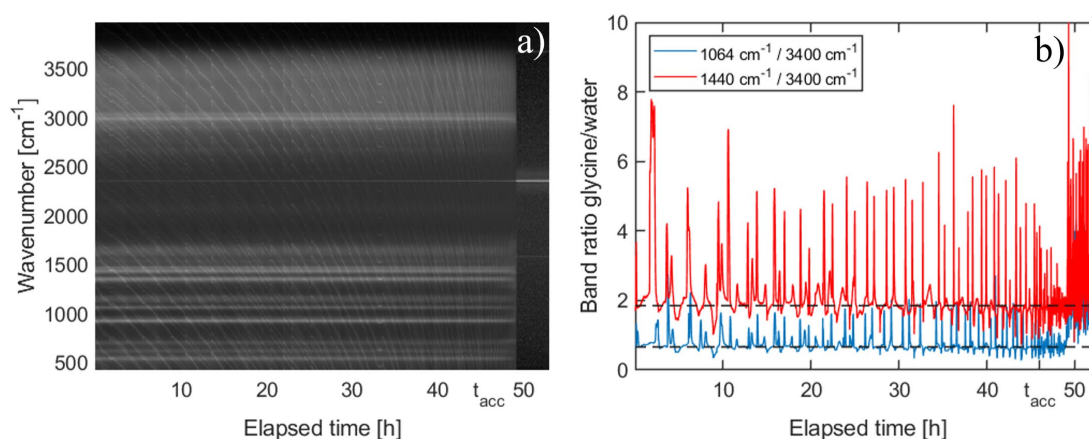
134 To gain further insight into the shrinking mechanism, we analyze the evolution of the Raman spectra over the
135 course of the shrinking process. A representative example of such an evolution is shown in Fig. 6. For Raman
136 spectra of single spherical particles, so called morphology dependent resonances, or whispering gallery modes
137 (WGMs) (Oraevsky, 2002), are superimposed on the molecular signals. To separate the WGMs from the molecular
138 signal of interest, the Raman spectra are normalized and stacked in chronological order from left to right, as shown
139 in Fig. 6a. The WGMs show up as a manifold of thin slanted lines bending towards lower wavenumbers with
140 increasing time as the droplet shrinks. Molecular band positions on the other hand are independent of particle
141 size, and are identified as horizontal lines in the evolution of the Raman spectra.

142

143 From Fig. 6a it is evident that the molecular Raman signal remains qualitatively the same, indicating that no
144 significant change in the molecular composition takes place in the droplet over the course of the shrinking process.
145 This behavior is observed for all investigated droplets. Since the particle loses the major part of its volume during



146 the shrinking, this implies that glycine is removed from the droplet as a consequence of chemical reaction (*vide*
147 *infra*). As the water vapor pressure of the droplet is given by the surrounding RH of 77 % and therefore has to
148 remain constant, the removal of glycine from the droplet must be accompanied by the evaporation of water in
149 order to maintain the equilibrium glycine concentration. A quantitative analysis of the Raman spectrum (Fig. 6b)
150 reveals that the spectral intensity of glycine modes with respect to the O-H stretching mode of water remains
151 constant, confirming a constant concentration of glycine molecules during the shrinking process. The measure-
152 ment ends when the particle becomes too small for stable trapping, and therefore leaves the optical trap.
153



154
155 **Figure 6** Temporal evolution of Raman signal during droplet shrinking. **a)** Normalized Raman spectra stacked
156 chronologically from left to right. The molecular Raman bands are visible as horizontal straight white lines on the
157 dark background. The finer, slanted and curved lines correspond to whispering gallery modes. After approxi-
158 mately 49 h, the particle leaves the optical trap as it reaches a size that is too small for trapping, and only back-
159 ground is recorded. The band remaining afterwards at 2323 cm^{-1} corresponds to the nitrogen gas in the trapping
160 cell. **b)** Ratio of the molecular glycine bands centered at 1064 cm^{-1} and 1440 cm^{-1} to the water band at around
161 3400 cm^{-1} . Peaks and dips in the graphs correspond to spectra where a whispering gallery mode is superimposed
162 on the glycine signal and the water signal, respectively, and are not relevant for the molecular composition. The
163 dashed horizontal lines are a guide to the eye. In this example, the acceleration of the droplet shrinking is observed
164 at $t_{\text{acc}} = 46$ h. From this point in time onwards until the particle is lost, the faster shrinking leads to more frequent
165 WGMs perceived as an apparent increase of noise in the data.

166 The linear dependence of the shrinking rate on the light intensity (Fig. 5) proves that the observed shrinking is
167 induced by the laser light. This observation is intriguing as aqueous glycine is not known to absorb light in the
168 visible range, similar to other amino acids (Bhat and Dharmaprakash, 2002). Furthermore, the linear dependence
169 between shrinking rate and light intensity rules out the possibility of multiphoton absorption, which might other-
170 wise populate energetically excited states of glycine to induce chemical reactions.

171



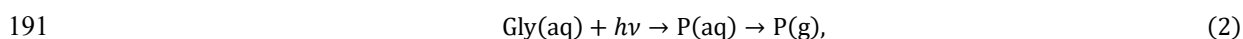
172 The observation of a constant shrinking rate over a large portion of the experiments (Fig. 4) provides another
173 important piece of information, as this allows us to rule out some of the possible shrinking mechanisms. For
174 instance, assuming some residual absorption of light at 532 nm by the droplet solution, one might argue that the
175 shrinking is a consequence of enhanced evaporation due to the droplet heating by the laser. The evaporation of
176 glycine from the droplet can be approximated by the Hertz-Knudsen equation:

$$177 \quad \frac{dN}{dt} = S \cdot \frac{\alpha p}{\sqrt{2\pi MRT}} \quad (1)$$

178 where $\frac{dN}{dt}$ is the molar evaporation rate of glycine, S is the droplet's surface, p is the partial pressure and M is the
179 molar mass of glycine, R the gas constant, T the temperature and α a heuristic sticking coefficient with values
180 between 0 and 1. It is evident from Eq. (1) that the rate of shrinking by evaporation should scale with the surface
181 area of the droplet, and that in this case a deceleration of the shrinking should be observed over time, contrary to
182 the experimental data. Moreover, any heating by laser light absorption would at most lead to a very small temper-
183 ature rise due to the efficient cooling by the gas flow. In addition to these arguments, if evaporation were signifi-
184 cant, some evaporation should still be observable even at low light intensity, where the heating of the droplet is
185 negligible and hence any deviations from room temperature can be neglected. As seen from Fig. 5 however, there
186 is no shrinking observable for low light intensities. We can therefore rule out evaporation as the dominant shrink-
187 ing mechanism.

188

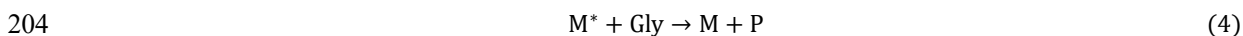
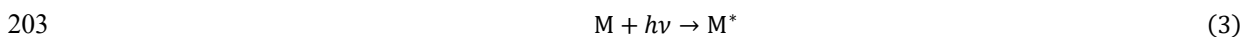
189 The observation of a constant shrinking rate also excludes photochemical reactions in which molecular glycine
190 directly absorbs photons:



192 where Gly(aq) is a solvated glycine molecule, $h\nu$ is the energy of the incoming photon and P is the reaction prod-
193 uct that is removed from the droplet (aq) into the surrounding gas phase (g) afterwards. As mentioned above,
194 molecular glycine is considered non-absorbing at 532 nm. However, if we nevertheless assume that molecular
195 glycine could be very weakly absorbing as in Eq. (2), the photon density inside the droplet would be constant over
196 the course of the photochemical reaction. Hence, the first step in Eq. (2) would be pseudo-first order, for which
197 the reaction rate is proportional to the concentration of glycine molecules in the droplet. Therefore, one would
198 expect a decrease in the observed shrinking rate over time, which contradicts the experimental observation.

199

200 The examples above illustrate that any mechanism, in which glycine molecules directly absorb incoming photons,
201 cannot explain the constant shrinking rates. This implies that a more intricate reaction must take place in the
202 droplet. We suggest the following simplified scheme with an additional reaction partner M:





205 where M^* denotes a photoexcited state of M , and P is the reaction product of glycine in the presence of this photoexcited species. This scheme represents a mediated reaction in which the reaction partner M is activated by light
206 absorption, and then reacts with glycine and returns back to the ground state. M shows the characteristics of a
207 photosensitizer (Corral Arroyo et al., 2018; George et al., 2015; Wang et al., 2020; Rapf and Vaida, 2016), which
208 is not consumed during the reaction, and therefore the amount of M remains constant in the droplet. We further
209 assume that the light absorption of the photosensitizer M is the rate limiting step, i.e., that Eq. (3) proceeds much
210 slower than Eq. (4). This is equivalent to requiring that M is only weakly absorbing, or that the concentration of
211 M in the droplet is low. Since the amount of M in the rate limiting step (Eq. (3)) remains constant during the
212 shrinking process, so does M^* (quasistationary), resulting in a constant rate of degradation of Gly (Eq. (4)). As-
213 suming that the absolute concentration of M is much smaller than that of Gly at all times, and therefore has no
214 relevant effect on the equilibrium water vapor pressure of the droplet, the volume shrinking rate is predicted to be
215 constant in accordance with the experimental data.
216

217

218 Although the proposed mechanism in Eq. (3) and (4) concurs with the observed constant shrinking rates, it does
219 not yet specify the nature of the photosensitizer and its reaction with glycine. We first discuss potential candidates
220 for the photosensitizer. Contamination during the preparation of the different aqueous glycine solutions used in
221 this study was minimized by using pure substances (glycine purity $\geq 99\%$, water resistivity $18.2\text{ M}\Omega\cdot\text{s}$). No
222 correlation between the shrinking rates in Fig. 5 and the age of the solution at the time of the measurements was
223 observed, which indicates that there is no accumulation of photoactive contaminants in the solution after the
224 preparation. We therefore argue that contamination is not the origin of the photosensitizer.
225

226

227 It is evident from the previous discussion that the photosensitizer must possess an absorption band at 532 nm,
228 which is not the case for single solvated glycine molecules. The optical properties of molecules may change
229 however when forming intermolecular bonds, e.g. leading to an enhancement of the absorption and fluorescence
230 in the case of protein aggregates (Homchaudhuri and Swaminathan, 2004; Shukla et al., 2004; Chan et al., 2013;
231 Pinotsi et al., 2013) and amino acid clusters (Chen et al., 2018). For glycine solutions in particular, observations
232 of light absorption in the near UV/vis range have been attributed to the presence of mesoscopic clusters (Jawor-
233 Baczynska et al., 2013; Zimbitas et al., 2019), specifically due to the formation of hydrogen bonds between indi-
234 vidual molecules (Terpugov et al., 2021).

235

236 Mesoscopic clusters occur naturally in both undersaturated and supersaturated glycine solutions, though a kinetic
237 barrier may have to be overcome for their formation (Jawor-Baczynska et al., 2013). The average size of the
238 mesoscopic clusters, typically of the order of 100 nm for bulk solutions, depends not only on the monomer con-
239 centration but also on the history of the sample, indicating that the clusters do not necessarily remain in thermo-
240 dynamic equilibrium after formation (Jawor-Baczynska et al., 2013). Based on these observations, we propose
that the photo-induced droplet shrinking is mediated by light absorption of mesoclusters in the glycine solution.

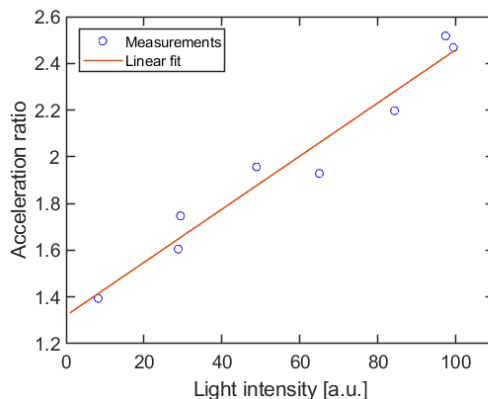


241 These mesoclusters remain kinetically stable during the droplet shrinking, despite the decrease of the absolute
242 number of glycine monomers (i. e. constant glycine monomer concentration). Hence, these clusters act as stable
243 photosensitizers inside the droplets, in accordance with the observed constant shrinking rate. The observation of
244 a constant initial shrinking rate thus allows us to narrow down the possible reaction mechanisms at work in the
245 droplets. Alternative schemes might be conceivable, such as the existence of several reaction partners for glycine.
246 However, there is no further experimental evidence in favor of more complex alternatives to the simple mecha-
247 nism proposed (Eq. (3) and (4)). Furthermore, as pointed out above, mesoscopic glycine clusters match the req-
248 uisite characteristics of the proposed photosensitizer, and are therefore likely candidates. To pursue the argument,
249 let us further discuss the role of the mesoscopic clusters in the observed acceleration of the droplet shrinking.

250

251 The acceleration of the droplet shrinking proceeds relatively promptly at the point of acceleration when the par-
252 ticle has lost a typical amount of 75 % of its volume (Fig. 4). Assuming that the total number of mesoclusters
253 remains approximately constant (M in Eqs.(3) and (4)), their concentration has increased by an approximate factor
254 of 4 at this point. The sudden nature of the shrinking acceleration hints at a phase transition inside the particle. In
255 particular, the increase in nanocluster concentration may trigger the separation of a dense cluster phase inside the
256 droplets as part of a liquid-liquid phase transition. While a definite conclusion has to await more detailed micro-
257 scopic investigations, we present the following arguments in favor of this explanation. Mesoscopic clusters in
258 aqueous solutions are known to interact with focused light irradiation by assembling in the focal point of the light
259 beam due to the optical force that acts on the individual clusters (Sugiyama et al., 2012). This mechanism is the
260 basis of laser-induced phase transitions(Alexander and Camp, 2019), in the particular case of glycine both for
261 liquid-liquid phase separation (Sugiyama et al., 2012; Yuyama et al., 2010) and solid crystal nucleation (Sugiyama
262 et al., 2012; Alexander and Camp, 2019; Yuyama et al., 2010; Zaccaro et al., 2001; Garetz et al., 2002). It should
263 be noted at this point that the spot size in the focus of our optical trap is slightly larger ($5\ \mu\text{m}$) than the typical
264 droplet size, and that therefore, it might appear unlikely that the electromagnetic field gradient is strong enough
265 to induce cluster aggregation in our case. However, micrometer sized droplets exhibit a large variance in the
266 spatial distribution of the internal light field, owing to the nanofocusing effect (Cremer et al., 2016; Corral Arroyo
267 et al., 2022), which can provide the field gradients necessary for aggregation. If in the case of our trapped droplets,
268 the acceleration is due to a phase transition, it would likely be assisted by the light irradiance. One would therefore
269 expect a dependence of the observed shrinking acceleration on the incident light intensity. Fig. 7 shows the meas-
270 ured acceleration ratio, that is, the ratio between the shrinking rate after to before the point of acceleration, as a
271 function of light intensity. From this data it is evident that the ratio increases with higher light intensity, which
272 agrees with our explanation of a light-induced phase transition. Since in this scheme, the clusters are expected to
273 aggregate in the regions of high light intensity after reaching a critical concentration, this would lead to a larger
274 absorption rate and thus a larger subsequent reaction rate, in agreement with the observation. Further studies will
275 be necessary to provide conclusive evidence for this explanation.

276



277

278 **Figure 7** Acceleration of droplet shrinking versus light intensity. The solid line represents the best linear fit
279 through the measurement data.

280 More data will also be required to understand the specifics of the interaction between the photosensitizer and the
281 solvated glycine molecules in Eq. (4). Here, we can only provide a qualitative discussion based on the available
282 data. The Raman spectra (Fig. 6) show no detectable change in the molecular composition, even after the droplet
283 has lost the major part of its volume during the shrinking process. Since this observation rules out the accumula-
284 tion of reaction products in the droplets over time, the reaction products must be small, volatile compounds that
285 quickly evaporate into the surrounding gas phase. Known degradation mechanisms of glycine and other amino
286 acids in aqueous solution proceed via reaction with radical species, in particular solvated electrons e_{solv}^- and hy-
287 droxyl $\cdot\text{OH}$ radicals (Moenig et al., 1985; Garrison, 1964, 1972), which form as part of a photosensitized reaction
288 with chromophoric organic matter in water (Lundeen et al., 2014; Sun et al., 2018; Mopper and Zika, 1987).
289 Currently, our data does not allow us to distinguish between different degradation pathways.

290

291 4. CONCLUSIONS

292 We have demonstrated that single micrometer sized aqueous glycine droplets respond to the illumination with
293 laser light of 532 nm by shrinking, despite the fact that molecular glycine does not absorb in the near UV/vis
294 range. Most remarkably, the volume shrinking rate remained constant over the major part of the shrinking process.
295 This indicates a photo-induced decay of glycine molecules in the presence of a rate limiting catalyst, or photosen-
296 sitizer, and the subsequent evaporation of small, volatile reaction products. Based on the available literature data,
297 we propose that intrinsic mesoscopic clusters of glycine molecules formed by hydrogen bonding in the aqueous
298 solution are the most plausible candidates for this photosensitizer. The presence of mesoscopic glycine clusters
299 would also explain the sudden acceleration of the shrinking rate occurring at a volume loss of $\sim 75\%$. Because of
300 its dependence on the light intensity, we attribute this sudden rate change to arise from the interaction of the
301 mesoclusters with the incident light, possibly initiating a light-induced phase transition.

302



303 This study provides yet another example of the non-trivial interactions of light with aqueous glycine solutions
304 (Alexander and Camp, 2019; Sugiyama et al., 2012; Zaccaro et al., 2001; Garetz et al., 2002; Yuyama et al., 2010),
305 which facilitate previously undiscovered reaction pathways - interactions that are likely not exclusive to glycine.
306 Light harvesting by and light interaction with such mesoscopic photosensitizers in aerosol droplets might also
307 have played a role in the formation of more complex organic molecules under prebiotic conditions. Further in-
308 vestigations are needed to shed light on the specifics of the observed phenomena, and to yield new insight into
309 the underlying reaction mechanisms, which remain elusive in part. Studying solutions in micrometer sized drop-
310 lets (attoliter volumes) using high laser powers offers the advantage of much higher sensitivity to photo-induced
311 reactions than typically achievable with bulk solutions.

312

313 **Acknowledgements**

314 This project was supported by the Japan Society for the Promotion of Science (JSPS Oversea Research Fellow-
315 ship; S.I.), by the Swiss National Science Foundation (SNSF project number 200020_200306), and by ETH Zü-
316 rich. We are very grateful to D. Stapfer and M. Steger from our workshops for technical support, and to D. Zindel
317 for helpful discussions.

318

319 **Data Repository**

320 The data that support our findings are deposited on the ETH Research Collection under <https://doi.org/xx>.

321



322 References

- 323 Alexander, A. J. and Camp, P. J.: Non-photochemical laser-induced nucleation, *The Journal of chemical physics*, 150, 040901, 2019.
- 324 Altaf, M. B., Zuend, A., and Freedman, M. A.: Role of nucleation mechanism on the size dependent morphology of organic aerosol, *Chem.*
325 *Commun.*, 52, 9220-9223, 2016.
- 326 Arnstein, H.: The metabolism of glycine, in: *Adv. Protein Chem.*, Elsevier, 1-91, 1954.
- 327 Ashkin, A.: Optical trapping and manipulation of neutral particles using lasers, *Proceedings of the National Academy of Sciences*, 94, 4853-
328 4860, 1997.
- 329 Bain, R. M., Sathyamoorthi, S., and Zare, R. N.: "On - droplet" chemistry: the cycloaddition of diethyl azodicarboxylate and quadricyclane,
330 *Angew. Chem.*, 129, 15279-15283, 2017.
- 331 Bhat, M. N. and Dharmaprakash, S.: Growth of nonlinear optical γ -glycine crystals, *J. Cryst. Growth*, 236, 376-380, 2002.
- 332 Bohren, C. F. and Huffman, D. R.: *Absorption and scattering of light by small particles*, John Wiley & Sons 2008.
- 333 Bones, D. L., Reid, J. P., Lienhard, D. M., and Krieger, U. K.: Comparing the mechanism of water condensation and evaporation in glassy
334 aerosol, *Proceedings of the National Academy of Sciences*, 109, 11613-11618, 2012.
- 335 Boucher, O., Randall, D., Artaxo, P., Bretherton, C., Feingold, G., Forster, P., Kerminen, V.-M., Kondo, Y., Liao, H., and Lohmann, U.:
336 Clouds and aerosols, in: *Climate change 2013: the physical science basis. Contribution of Working Group I to the Fifth Assessment*
337 *Report of the Intergovernmental Panel on Climate Change*, Cambridge University Press, 571-657, 2013.
- 338 Bzdek, B. R. and Reid, J. P.: Perspective: Aerosol microphysics: From molecules to the chemical physics of aerosols, *The Journal of*
339 *Chemical Physics*, 147, 220901, 2017.
- 340 Chan, F. T., Schierle, G. S. K., Kumita, J. R., Bertoncini, C. W., Dobson, C. M., and Kaminski, C. F.: Protein amyloids develop an intrinsic
341 fluorescence signature during aggregation, *Analyst*, 138, 2156-2162, 2013.
- 342 Chan, M. N., Choi, M. Y., Ng, N. L., and Chan, C. K.: Hygroscopicity of water-soluble organic compounds in atmospheric aerosols: Amino
343 acids and biomass burning derived organic species, *Environ. Sci. Technol.*, 39, 1555-1562, 2005.
- 344 Chen, X., Luo, W., Ma, H., Peng, Q., Yuan, W. Z., and Zhang, Y.: Prevalent intrinsic emission from nonaromatic amino acids and poly
345 (amino acids), *Science China Chemistry*, 61, 351-359, 2018.
- 346 Čižmár, T., Garcés-Chávez, V., Dholakia, K., and Zemánek, P.: Optical conveyor belt for delivery of submicron objects, *Appl. Phys. Lett.*,
347 86, 174101, 2005.
- 348 Corral Arroyo, P., David, G., Alpert, P. A., Parmentier, E. A., Ammann, M., and Signorell, R.: Amplification of light within aerosol particles
349 accelerates in-particle photochemistry, *Science*, 376, 293-296, 2022.
- 350 Corral Arroyo, P., Bartels-Rausch, T., Alpert, P. A., Dumas, S. p., Perrier, S. b., George, C., and Ammann, M.: Particle-phase photosensitized
351 radical production and aerosol aging, *Environ. Sci. Technol.*, 52, 7680-7688, 2018.
- 352 Cremer, J. W., Thaler, K. M., Haisch, C., and Signorell, R.: Photoacoustics of single laser-trapped nanodroplets for the direct observation of
353 nanofocusing in aerosol photokinetics, *Nature communications*, 7, 1-7, 2016.
- 354 David, G., Parmentier, E. A., Taurino, I., and Signorell, R.: Tracing the composition of single e-cigarette aerosol droplets in situ by laser-
355 trapping and Raman scattering, *Scientific reports*, 10, 1-8, 2020.
- 356 Esat, K., David, G., Poulkas, T., Shein, M., and Signorell, R.: Phase transition dynamics of single optically trapped aqueous potassium
357 carbonate particles, *Physical Chemistry Chemical Physics*, 20, 11598-11607, 2018.
- 358 Garetz, B. A., Matic, J., and Myerson, A. S.: Polarization switching of crystal structure in the nonphotochemical light-induced nucleation of
359 supersaturated aqueous glycine solutions, *Phys. Rev. Lett.*, 89, 175501, 2002.
- 360 Garrison, W. M.: Actions of ionizing radiations on nitrogen compounds in aqueous media, *Radiation Research Supplement*, 4, 158-174,
361 1964.
- 362 Garrison, W. M.: *Radiation-induced reactions of amino acids and peptides*, Univ. of California, Berkeley, 1972.
- 363 George, C., Ammann, M., D'Anna, B., Donaldson, D., and Nizkorodov, S. A.: Heterogeneous photochemistry in the atmosphere, *Chem.*
364 *Rev.*, 115, 4218-4258, 2015.
- 365 Girod, M., Moyano, E., Campbell, D. I., and Cooks, R. G.: Accelerated bimolecular reactions in microdroplets studied by desorption
366 electrospray ionization mass spectrometry, *Chemical Science*, 2, 501-510, 2011.
- 367 Gong, Z., Pan, Y.-L., Videen, G., and Wang, C.: Optical trapping and manipulation of single particles in air: Principles, technical details,
368 and applications, *J. Quant. Spectrosc. Radiat. Transfer*, 214, 94-119, 2018.
- 369 Hall, J. C.: Glycine, *Journal of Parenteral and Enteral Nutrition*, 22, 393-398, 1998.
- 370 Homchaudhuri, L. and Swaminathan, R.: Near ultraviolet absorption arising from lysine residues in close proximity: a probe to monitor
371 protein unfolding and aggregation in lysine-rich proteins, *Bull. Chem. Soc. Jpn.*, 77, 765-769, 2004.
- 372 Jackson, A. A.: The glycine story, *Eur J Clin Nutr*, 45, 59-65, 1991.
- 373 Jawor-Baczynska, A., Moore, B. D., Lee, H. S., McCormick, A. V., and Sefcik, J.: Population and size distribution of solute-rich mesospecies
374 within mesostructured aqueous amino acid solutions, *Faraday Discuss.*, 167, 425-440, 2013.
- 375 Kucinski, T. M., Dawson, J. N., and Freedman, M. A.: Size-Dependent Liquid-Liquid Phase Separation in Atmospherically Relevant
376 Complex Systems, *The Journal of Physical Chemistry Letters*, 10, 6915-6920, 2019.
- 377 Lee, J. K., Banerjee, S., Nam, H. G., and Zare, R. N.: Acceleration of reaction in charged microdroplets, *Q. Rev. Biophys.*, 48, 437-444,
378 2015.
- 379 Lee, J. K., Samanta, D., Nam, H. G., and Zare, R. N.: Micrometer-sized water droplets induce spontaneous reduction, *Journal of the American*
380 *Chemical Society*, 141, 10585-10589, 2019.
- 381 Lundeen, R. A., Janssen, E. M.-L., Chu, C., and McNeill, K.: Environmental photochemistry of amino acids, peptides and proteins, *CHIMIA*
382 *International Journal for Chemistry*, 68, 812-817, 2014.
- 383 Moenig, J., Chapman, R., and Asmus, K. D.: Effect of the protonation state of the amino group on the cnddot. OH radical induced
384 decarboxylation of amino acids in aqueous solution, *The Journal of Physical Chemistry*, 89, 3139-3144, 1985.
- 385 Mopper, K. and Zika, R. G.: Natural photosensitizers in sea water: riboflavin and its breakdown products, in: *ACS Publications*, 1987.
- 386 Oraevsky, A. N.: Whispering-gallery waves, *Quantum electronics*, 32, 377, 2002.



- 387 Parmentier, E. A., Corral Arroyo, P., Gruseck, R., Ban, L., David, G., and Signorell, R.: Charge Effects on the Photodegradation of Single
388 Optically Trapped Oleic Acid Aerosol Droplets, *The Journal of Physical Chemistry A*, 126, 4456-4464, 2022.
- 389 Pinotsi, D., Buell, A. K., Dobson, C. M., Kaminski Schierle, G. S., and Kaminski, C. F.: A label - free, quantitative assay of amyloid fibril
390 growth based on intrinsic fluorescence, *ChemBioChem*, 14, 846-850, 2013.
- 391 Pöschl, U. and Shiraiwa, M.: Multiphase chemistry at the atmosphere–biosphere interface influencing climate and public health in the
392 anthropocene, *Chem. Rev.*, 115, 4440-4475, 2015.
- 393 Rapf, R. J. and Vaida, V.: Sunlight as an energetic driver in the synthesis of molecules necessary for life, *Physical Chemistry Chemical
394 Physics*, 18, 20067-20084, 2016.
- 395 Reich, O., David, G., Esat, K., and Signorell, R.: Weighing picogram aerosol droplets with an optical balance, *Communications Physics*, 3,
396 223, 10.1038/s42005-020-00496-x, 2020.
- 397 Ruiz-Lopez, M. F., Francisco, J. S., Martins-Costa, M. T., and Anglada, J. M.: Molecular reactions at aqueous interfaces, *Nature Reviews
398 Chemistry*, 4, 459-475, 2020.
- 399 Shukla, A., Mukherjee, S., Sharma, S., Agrawal, V., Kishan, K. R., and Guptasarma, P.: A novel UV laser-induced visible blue radiation
400 from protein crystals and aggregates: scattering artifacts or fluorescence transitions of peptide electrons delocalized through hydrogen
401 bonding?, *Arch. Biochem. Biophys.*, 428, 144-153, 2004.
- 402 Sugiyama, T., Yuyama, K.-i., and Masuhara, H.: Laser trapping chemistry: from polymer assembly to amino acid crystallization, *Acc. Chem.
403 Res.*, 45, 1946-1954, 2012.
- 404 Sun, Z., Zhang, C., Xing, L., Zhou, Q., Dong, W., and Hoffmann, M. R.: UV/nitrotriacetic acid process as a novel strategy for efficient
405 photoreductive degradation of perfluorooctanesulfonate, *Environ. Sci. Technol.*, 52, 2953-2962, 2018.
- 406 Swietlicki, E., Hansson, H. C., Hämeri, K., Svenningsson, B., Massling, A., McFiggans, G., McMurry, P. H., Petäjä, T., Tunved, P., Gysel,
407 M., Topping, D., Weingartner, E., Baltensperger, U., Rissler, J., Wiedensohler, A., and Kulmala, M.: Hygroscopic properties of
408 submicrometer atmospheric aerosol particles measured with H-TDMA instruments in various environments—a review, *Tellus B:
409 Chemical and Physical Meteorology*, 60, 432-469, 10.1111/j.1600-0889.2008.00350.x, 2008.
- 410 Tang, I. N., Tridico, A. C., and Fung, K. H.: Thermodynamic and optical properties of sea salt aerosols, *Journal of Geophysical Research:
411 Atmospheres*, 102, 23269-23275, 10.1029/97jd01806, 1997.
- 412 Terpugov, E. L., Kondratyev, M. S., and Degtyareva, O. V.: Light-induced effects in glycine aqueous solution studied by Fourier transform
413 infrared-emission spectroscopy and ultraviolet-visible spectroscopy, *J. Biomol. Struct. Dyn.*, 39, 108-117, 2021.
- 414 Tervahattu, H., Tuck, A., and Vaida, V.: Chemistry in prebiotic aerosols: a mechanism for the origin of life, in: *Origins*, Springer, 153-165,
415 2004.
- 416 Walsler, M. L., Park, J., Gomez, A. L., Russell, A. R., and Nizkorodov, S. A.: Photochemical aging of secondary organic aerosol particles
417 generated from the oxidation of d-limonene, *The Journal of Physical Chemistry A*, 111, 1907-1913, 2007.
- 418 Wang, X., Gemayel, R., Hayeck, N., Perrier, S., Charbonnel, N., Xu, C., Chen, H., Zhu, C., Zhang, L., and Wang, L.: Atmospheric
419 photosensitization: a new pathway for sulfate formation, *Environ. Sci. Technol.*, 54, 3114-3120, 2020.
- 420 Yuyama, K.-i., Sugiyama, T., and Masuhara, H.: Millimeter-scale dense liquid droplet formation and crystallization in glycine solution
421 induced by photon pressure, *The Journal of Physical Chemistry Letters*, 1, 1321-1325, 2010.
- 422 Zaccaro, J., Matic, J., Myerson, A. S., and Garetz, B. A.: Nonphotochemical, laser-induced nucleation of supersaturated aqueous glycine
423 produces unexpected γ -polymorph, *Crystal Growth & Design*, 1, 5-8, 2001.
- 424 Zieger, P., Väisänen, O., Corbin, J. C., Partridge, D. G., Bastelberger, S., Mousavi-Fard, M., Rosati, B., Gysel, M., Krieger, U. K., Leck, C.,
425 Nenes, A., Riipinen, I., Virtanen, A., and Salter, M. E.: Revising the hygroscopicity of inorganic sea salt particles, *Nature
426 Communications*, 8, 15883, 10.1038/ncomms15883, 2017.
- 427 Zimbitas, G., Jawor-Baczynska, A., Vesga, M. J., Javid, N., Moore, B. D., Parkinson, J., and Sefcik, J.: Investigation of molecular and
428 mesoscale clusters in undersaturated glycine aqueous solutions, *Colloids Surf. Physicochem. Eng. Aspects*, 579, 123633, 2019.

429